



Use of Cardiac Imaging to Evaluate Cardiac Function and Pulmonary Hemodynamics in Patients with Heart Failure

Tomoko S. Kato^{1,2} · Masao Daimon^{3,4} · Toru Satoh⁵

Published online: 10 May 2019
© Springer Science+Business Media, LLC, part of Springer Nature 2019

Abstract

Purpose of Review Noninvasive hemodynamic assessments in patients with heart failure (HF) are essential for appropriate diagnosis and establishment of the best treatment strategies. Recently, the impact of pulmonary circulation and right ventricular function on prognosis in HF patients has drawn increasing attention. In this article, we explore the usefulness of cardiac imaging for hemodynamic assessments, mainly focusing on echocardiographic evaluation.

Recent Findings The reliability of Doppler echocardiography as a noninvasive alternative to Swan-Ganz catheterization has been well investigated with higher than 80% accuracy for estimating pulmonary artery pressure. Strain measurement and three-dimensional echocardiography are useful for evaluating right ventricular function together with pulmonary circulation. The accuracy of analyzing left and right ventricular functions by cardiac computed tomography and cardiac magnetic resonance imaging has also been established. These modalities can provide myocardial tissue information and allow calculation of the extracellular volume fraction as well.

Summary According to the rapid improvement of technologies, cardiac imaging has become an essential tool for hemodynamic evaluation in HF management.

Keywords Echocardiography · Cardiac computed tomography · Cardiac magnetic resonance imaging · Noninvasive monitoring · Hemodynamics · Heart failure

Introduction

The prevalence of patients with cardiovascular disease, especially those with heart failure (HF), has dramatically increased in recent years. HF affects an estimated 26 million people worldwide, and 1–2% of healthcare budgets have been spent on heart failure over recent decades [1, 2]. Frequent hospitalization of HF patients and its huge economic burden to society

can be reduced if HF treatments can be practically optimized by noninvasive hemodynamic assessments, such as echocardiography and other cardiac imaging modalities, instead of right heart catheterization. In addition, evaluation of cardiac function by imaging modalities can provide not only hemodynamic information but also chamber morphological information. This would be a significant advantage of cardiac imaging tools over right heart catheterization.

This article is part of the Topical Collection on *Heart Failure*

✉ Tomoko S. Kato
rinnko@sannet.ne.jp

Masao Daimon
daimon@muf.biglobe.ne.jp

Toru Satoh
tsatoh@ks.kyorin-u.ac.jp

¹ Department of Medicine, Division of Cardiology, Showa University Koto Toyosu Hospital, 5-1-38 Toyosu, Koto-ku, Tokyo 135-8577, Japan

² Department of Cardiovascular Medicine, Juntendo University School of Medicine, Tokyo, Japan

³ Department of Cardiovascular Medicine, The University of Tokyo Hospital, Tokyo, Japan

⁴ Department of Clinical Laboratory, The University of Tokyo Hospital, Tokyo, Japan

⁵ Department of Cardiovascular Medicine, Kyorin University, Tokyo, Japan

Although a majority of patients with HF require hospitalization due to congestion, several trials of devices monitoring changes in the volume status of HF patients did not prove the effect of reducing hospitalizations [3, 4]. On the other hand, elevations of pulmonary artery pressure (PAP) and pulmonary vascular resistance (PVR) have been recognized as independent predictors for poor prognosis, not only in patients with pulmonary arterial hypertension (PAH) but also in patients with left-sided HF [5–8]. Frequent monitoring of PAP significantly reduces HF hospitalization rates [6]. However, of note, we should not only focus on PAP but also pay attention to right ventricular (RV) function [9]. The left ventricle (LV) has the capacity to generate high pressure with its contractile reserve when the afterload increases, whereas the RV has a very limited capacity to produce enough pressure against its high afterload [10]. The RV has a compensatory mechanism against the elevated afterload, such as contractive force reinforcement by RV myocardium hypertrophy, reduction of wall stress by shape change, and chamber enlargement to handle a larger preload. Even so, when RV is exposed to a high afterload condition for a prolonged time, the oxygen supply-demand mismatch in hypertrophic RV myocardium and the dilatation of the RV cause the interventricular septum to shift toward the left and gradually reduce RV contractility. The pressure that

generates the force of the ventricles is mainly produced by the chamber twisting, which depends on oblique muscle and transverse muscle contractions. However, an RV free wall lacks oblique muscle, and its longitudinal shortening contributes to overall RV function under normal afterload conditions [11]. Under a condition of high PAP, a septal wall portion of the RV also contributes to generating pressure for pulmonary circulation; however, excessive PA elevations change the septal shape, which drastically reduces the ejection power of RV. Therefore, in patients who have encountered progressive RV failure caused by long-standing excessive afterload, their RVs lose the ability to generate pressure and the PAP may decrease as a consequence of low cardiac output [9]. Therefore, we should evaluate both PAP and the degree of RV dysfunction accompanied with RV morphological change in HF patients at the same time.

Ghio et al. revealed the necessity of combining the right heart hemodynamic variables with a functional evaluation of the RV for risk stratification of patients with HF [5]. They showed that increased PAP accompanied with reduced RV ejection fraction (RVEF) was clinically associated with significantly poorer prognosis than having neither condition (Fig. 1A). Sub-analysis of BEST (beta-blocker evaluation of survival trial) also revealed that reduced RVEF is a significant independent predictor of

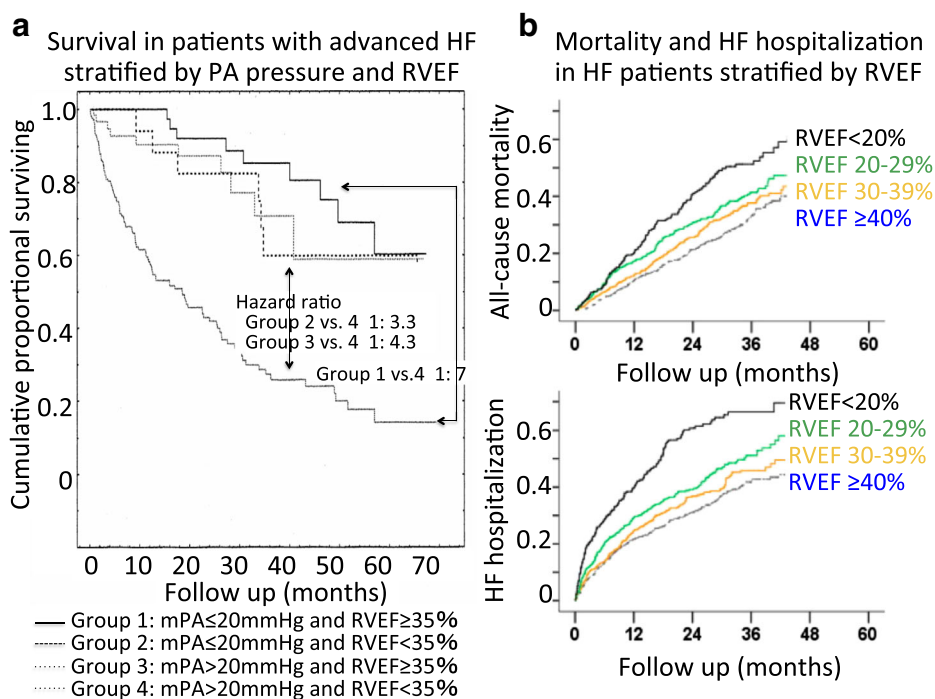


Fig. 1 a Survival rates in patients with advanced heart failure, grouped according to the coupling between mean pulmonary artery pressure (PAP) and right ventricular ejection fraction (RVEF). Group 1, normal PAP/preserved RVEF ($n = 73$); group 2, normal PAP/low RVEF ($n = 68$); group 3, high PAP/preserved RVEF ($n = 21$); group 4, high PAP/low

RVEF ($n = 215$) (reproduced from Ghio et al. *J Am Coll Cardiol* 2001;37:183–8, with permission from Elsevier) [5]. **b** Kaplan–Meier plots for all-cause mortality (upper) and HF hospitalization (lower) by RVEF categories (reproduced from Meyer et al. *Circulation* 2010;121:252–8, with permission from Wolters Kluwer Health, Inc.) [12]

mortality and hospitalization in patients with systolic HF [12] (Fig. 1a). Regarding RV morphology, Brown et al. reported that longitudinal shortening of RV accounts for the majority of RV contractility and improvement of RV function following pulmonary vasodilator therapy occurs from improvements in longitudinal contractions [11].

From the above points of view, it seems important to make excellent use of cardiac imaging modalities in order to evaluate cardiac function in a comprehensive manner that includes pulmonary circulation and RV functional analysis. In this review article, we provide an overview of imaging modality-derived noninvasive hemodynamic assessment, mostly highlighting the recent development of quantitative echocardiographic evaluation. We also summarize the recent investigations regarding pulmonary circulatory hemodynamics and RV functional evaluation by imaging modalities.

Assessment of Cardiac Function Using Echocardiography

Hemodynamic Evaluation by Echocardiography

Doppler echocardiography is now recognized as a reliable and cost-effective noninvasive alternative to right heart catheterization for hemodynamic assessment. Most of these measurements, including right atrial pressure (RAP), PAP, and cardiac output (CO), are easily obtainable at the bedside. Echocardiographic hemodynamic assessment is now used as a guide for treatment optimization and decision-making for medical or surgical therapy. It may be also used to monitor critically ill patients.

Several studies have demonstrated a good correlation between hemodynamic parameters obtained from echocardiography and those derived from invasive measurements. Various echocardiographic methods have been suggested for evaluation of each parameter, but their accuracy varies between the studies and may not be applicable in certain situations. Most commonly used methodologies for hemodynamic assessment by echocardiography, which are supported by the current guidelines [13••, 14] and described in recent studies [15–19], are summarized in Table 1.

RAP or central venous pressure (CVP) estimation by echocardiography would be the most frequently used in a setting of daily clinical practice. Evaluation of inferior vena cava (IVC) diameter and collapsibility can be relatively easily obtained at the subcostal window from any patients, and it would help identify patients who are in hypovolemic states. Of note, IVC collapsibility would not occur in patients supported by positive airway pressure ventilation, and it should not be used for RAP estimation [13••]. CO and stroke volume (SV) are the most important targets for optimization of hemodynamics in patients with cardiovascular disease, and echo-derived

noninvasive assessments should guide treatment strategy. Since the CO calculation by echocardiography was first reported by Magnin et al. [20], a good correlation between invasive and echo-derived measurements has been shown in several studies and guidelines [13••, 15, 16]. Even so, the formula of CO and SV estimations includes the LV outflow (LVOT) diameter for calculating cross-section area, and an accurate calculation of LVOT is difficult in some patients because it varies between the echo-views. In addition, the LVOT shape is not a perfect circle. Therefore, repeated measurements of intra-patient changes in echo-derived CO and SV would be the most practical usage of this modality, which helps evaluate patient responses to medical or surgical therapy. Using echo-derived hemodynamic estimation as a tool to monitor “intra-patient” responsiveness to the treatments should be also applied to PAP, PVR, and SVR.

It is worth mentioning that estimation of CO at the RV outflow (RVOT) is an important parameter in the care of patients supported by left ventricular assist devices (LVAD). LVAD therapy has become a standard therapy for patients with advanced HF, not only as a bridge to cardiac transplantation but also as a destination therapy or a bridge to myocardial recovery. In patients supported by LVAD, systemic circulatory output, or combined LVAD and native heart-driven CO, is calculated using the RVOT diameter and the time-integral velocity of RVOT, according to the same formula as CO calculation at LVOT. Systemic circulatory output is the sum of a patient’s own cardiac output from the LV, when his or her aortic valve opens at least intermittently, and the flow from the LVAD. In other words, CO measured at RVOT minus the LVAD pump flow is equivalent to CO which a patient’s own heart can produce, as long as a patient does not have an intra-cardiac shunt [21]. Noninvasive measurement of systemic circulatory output and estimation of output from the own LV in patients supported by LVAD are critically important, not only for the optimization of LVAD settings but also for consideration of the timing of weaning from LVAD and the assessment of LVAD malfunction.

Serial assessments of PAP by echocardiography using tricuspid regurgitation (TR) jet velocity for calculation of the pressure gradient between RV and RA are also widely used in daily practice. This measurement is easily obtainable because most of patients with cardiovascular diseases or HF have some TR, and recent studies have proven its reliability in diagnosing pulmonary hypertension (PH) [7, 22]. Figure 2 shows an estimation of PAP by echocardiography. One of the critical roles of echo-derived noninvasive assessment of PAP is that the presence of PH is significantly associated with poor prognosis not only in patients with HF [5–8] but also in the general population [23]. Considering the recent progress of HF treatments, which have specifically targeted PH treatment, repeatable assessments of PAP using noninvasive methods would be required for optimization of treatment strategy [24].

Table 1 Evaluation of hemodynamic parameters by echocardiography

Hemodynamic parameter	Echocardiographic indices required for the assessment	Methodology/formula
RAP (mmHg)	IVC diameter	RAP \approx 0–5 mmHg; size < 2.1 cm, collapses > 50%
CVP (mmHg)	IVC diameter change with respiration (collapsibility)	RAP \approx 5–10 mmHg; size > 2.1 cm; collapses > 50%
	Venous flow pattern in SVC or hepatic vein, jugular vein	RAP \approx 10–20 mmHg; size > 2.1 cm; collapses < 50%
	Tricuspid inflow E	RAP > 8 mmHg; systolic wave (V_s) < diastolic wave (V_d)
	TDI-derived RV free wall e'	RAP > 10 mmHg; $E/e' > 6$
	Tricuspid inflow E	RAP = $-1.263 + 0.01116 \times [\text{acceleration rate (cm/s}^2\text{) of } E]$
Systolic PAP (mmHg)	TR jet maximal velocity	$sPAP \approx 4 \times TRV_{\max}^2 + RAP$
Mean PAP (mmHg)	TR jet tracing	$mPAP \approx (\text{mean PG obtained by TR jet}) + RAP$
	PR jet maximal velocity	$mPAP \approx 4 \times PRV_{\max}^2 + RAP$
Diastolic PAP (mmHg)	PR jet end-diastolic velocity	$mPAP \approx 4 \times PRV_{\text{diastolic end}}^2 + RAP$
PVR (WU)	TR jet maximal velocity	$PVR \approx TRV_{\max} \cdot TVI_{RVOT} \times 10 + 0.16$
	TVI of the RV outflow tract	$PVR > 6$ WU; $TRV_{\max}/TVI_{RVOT} > 0.275$
		$PVR \approx 5.19 \times TRV_{\max}^2/TVI_{RVOT} - 0.4$ (for patients with elevated PVR)
	Pulmonary systolic flow	$PVR \approx [(PEP_p - AcT_p)] / TT_p$
LAP (mmHg)	Mitral inflows E and A	Under normal global LV function (LVEF > 40%)
PCWP (mmHg)	TDI-derived mitral annular e'	PCWP ≤ 12 mmHg; $E/e' \leq 8$
		PCWP > 12 mmHg; $E/e' \geq 13$ (mean)
		PCWP > 12 mmHg; septal $E/e' \geq 15$, lateral $E/e' \geq 12$
		Depressed LV function (LVEF < 40%)
		PCWP ≤ 12 mmHg; $E/A < 1$, $E < 50$ cm/s
		PCWP > 12 mmHg; $E/A > 1$, DcT of $E < 150$ ms
	Mitral inflows E and A	$PCWP \approx 32.16 + (-0.1045 \times E) + (0.1345 \times A) + (-0.17 \times DcT \text{ of } E) + (4.95 \times E/A)$
SV (L)	TVI of the LV outflow tract	$SV \approx (R_{LVOT}/2)^2 \times TVI_{LVOT}$
	LV outflow diameter	
CO (L/min)	Heart rate	$CO \approx HR \times (R_{LVOT})^2 \times TVI_{LVOT}$
	TVI of the LV outflow tract	
	LV outflow diameter	
SVR (WU)	MR jet maximal velocity	$PVR \approx 0.459 + 49.397 \times (MRV_{\max} \cdot TVI_{LVOT})$
CO of the diseased LV under LVAD support (L/min)	Heart rate	CO of native LV $\approx [HR \times (R_{RVOT})^2 \times TVI_{RVOT}] - \text{estimated LVAD pump flow}$
	TVI of the RV outflow tract	
	RV outflow diameter	

RAP, right atrial pressure; CVP, central venous pressure; SVC, superior vena; TDI, tissue Doppler imaging; TR, tricuspid regurgitation; sPAP, mean pulmonary artery pressure; TRV_{\max} , peak velocity of tricuspid regurgitation jet; mPAP, mean pulmonary artery pressure; PG, pressure gradient; PR, pulmonary regurgitation; PRV_{\max} , peak velocity of pulmonary regurgitation jet; $PRV_{\text{diastolic end}}$, end-diastolic velocity of pulmonary regurgitation jet; TVI, time-velocity integral; TVI_{RVOT} , time-velocity integral of the right ventricular outflow tract; PEP_p , pre-ejection period of pulmonary systolic flow; AcT_p , acceleration time of pulmonary systolic flow; TT_p , total systolic time of pulmonary systolic flow; LAP, left atrial filling pressure; PCWP, pulmonary capillary wedge pressure; LV, left ventricular; LVEF, left ventricular ejection fraction; DcT , deceleration time; SV, stroke volume; CO, cardiac output; HR, heart rate; R_{LVOT} , LV outflow diameter; MRV_{\max} , peak velocity of mitral regurgitation jet; LVAD, left ventricular assist device

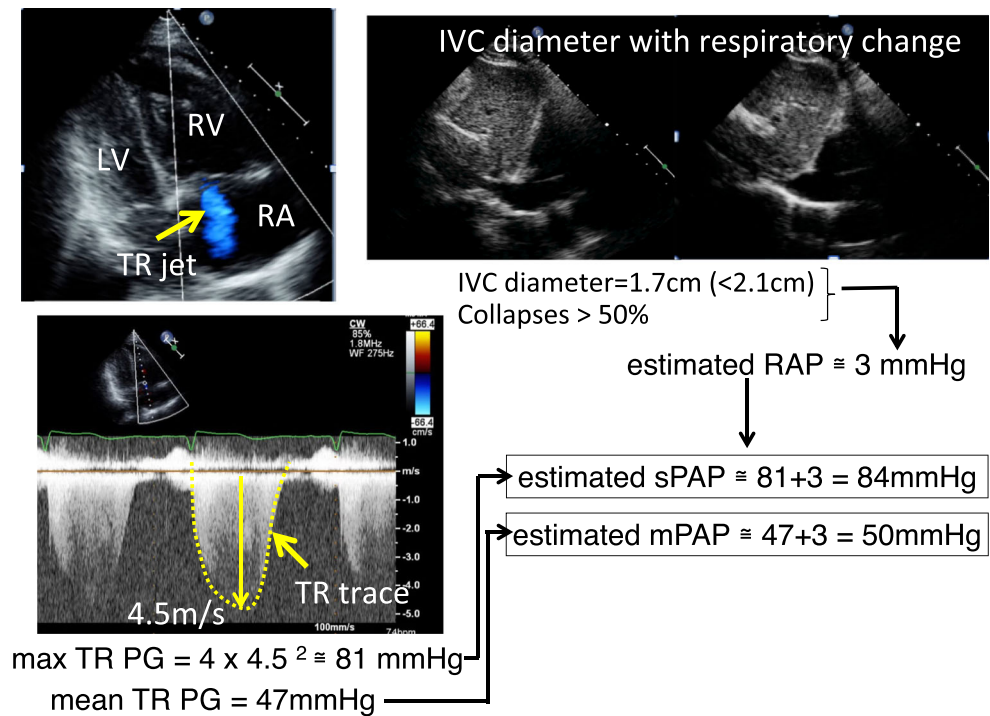
Reproduced and modified from Beigel R, et al. J Crit Care 2014;29:184.e1–8, with permission from Elsevier [15]

Assessment of Pulmonary Hypertension Due to Heart Failure by Echocardiography

The significant merit of noninvasive PAP assessment by echocardiography is that it can simultaneously evaluate LV diastolic function, which would help deduce PH types. Although the echo-derived estimation of hemodynamic parameters as continuous variables, especially regarding pulmonary capillary wedge pressure (PCWP), contains limitations, and the methodology itself has not yet been

fully validated, simultaneous evaluation of hemodynamics and ventricular function by echocardiography can provide physician with some hints for differentiating PH patients with isolated post-capillary PH (Ipc-PH) from those with combined post-capillary and pre-capillary PH (Cpc-PH) due to left-sided HF. Ipc-PH presents a hemodynamic state that is similar to what was previously known as passive post-capillary PH. Cpc-PH presents a hemodynamic state that is similar to what was previously known as reactive post-capillary PH.

Fig. 2 Evaluation of pulmonary artery pressure (PAP) by echocardiography. The upper right image demonstrates normal right atrial pressure of 3 mmHg. The lower image demonstrates the estimation of systolic PAP and mean PAP, based on the RV-RA pressure gradient (PG) using TR jet maximal velocity and TR jet trace. sPAP indicates systolic PAP



The current hemodynamic definition of PH is summarized in Table 2 [25••]. As stated above, group 2 PH, known as PH owing to the result of left heart disease, is classified into two different hemodynamic profiles. Previously, it was dichotomized to passive and reactive post-capillary PH using a transpulmonary gradient (TPG) defined as the mean PAP minus PCWP for discrimination; passive post-capillary PH was associated with $TPG \leq 12$ mmHg and reactive post-capillary PH was associated with $TPG > 12$ mmHg. Thereafter, the definition and the terminologies were updated, including the use of the diastolic pressure gradient (DPG), defined as diastolic PAP minus mean PAWP [25••]. Very recently, a proposal to change the diagnostic criteria of pulmonary hypertension from mean PAP > 25 mmHg to > 20 mmHg was made at the World Symposium on Pulmonary Hypertension in 2018. Thus, the cutoff values and the definition may possibly be altered in the near future, although the fundamental concept has been well investigated.

In Ipc-PH or passive post-capillary PH, high PCWP due to stiff LV with abnormal relaxation and compliance is transmitted back to the pulmonary venous circulation. The PAP elevation in passive PH patients is caused in order to produce forward flow from the pulmonary circulation to left atrium (LA); accordingly, a $TPG \leq 12$ mmHg or $DPG < 7$ mmHg is good enough. Stated differently, the degree of PA elevation in Ipc-PH patients is not extremely significant and can be reduced if LV diastolic function improves and PCWP decreases via adequate HF treatment. In contrast, Cpc-PH, which used to be called as

reactive PH or out-of-proportion PH, is associated with further significantly elevated PAPs that are conducive to vascular proliferative changes and vasoconstriction in both pulmonary venous and atrial systems. Patients in this category manifest with a pre-capillary component to PH, showing $TPG > 12$ mmHg or $DPG \geq 7$ mmHg. Due to histological changes in the pulmonary vasculature, elevated PAP in Cpc-PH patients cannot be normalized with treatment of underlying HF alone.

Accordingly, patients with post-capillary PH due to significantly advanced diastolic dysfunction are subjected to a pre-capillary component of PH and ultimately develop RV failure, which mimics RV structural and functional changes seen in patients with PAH (group 1 PH). From this point of view, echocardiography is a powerful tool for evaluating patients with HF and diastolic dysfunction who are at risk of or on the way to developing Cpc-PH. Their RV would initially show hypertrophy in response to the high afterload, followed by the development of RV and RA dilatations with leftward displacement of interventricular septum, so-called D-shaped LV. The disease progression gradually causes irreversible RV systolic and diastolic dysfunction. RV myocardial ischemia, owing to imbalanced oxygen demand and supply, occurs as a result of reduced coronary flow under elevated PAP. The reduced coronary flow cannot provide enough oxygen to hypertrophic and dilated RV and is reported to be a contributor to RV dysfunction in PH patients [26]. Figure 3 shows echocardiographic findings obtained from patients developing Cpc-PH.

Table 2 Hemodynamic definitions of pre- and post-capillary pulmonary hypertension

Definition	Characteristics*	Clinical group(s)**
PH	mPAP ≥ 25 mmHg	All
Pre-capillary PH	mPAP ≥ 25 mmHg PCWP ≤ 15 mmHg	1. Pulmonary arterial hypertension 3. PH due to lung diseases 4. Chronic thromboembolic PH
Post-capillary PH	mPAP ≥ 25 mmHg PCWP > 15 mmHg	2. PH due to left heart disease 5. PH with unclear and/or multifactorial mechanisms
Recent classification of post-capillary PH		
Using DPG Isolated post-capillary PH (Ipc-PH)	DPG < 7 mmHg and/or PVR ≤ 3 WU¶	2. PH due to left heart disease 5. PH with unclear and/or multifactorial mechanisms
Combined post-capillary and pre-capillary PH (Cpc-PH)	DPG ≥ 7 mmHg and/or PVR > 3 WU¶	2. PH due to left heart disease 5. PH with unclear and/or multifactorial mechanisms
Reactive post-capillary PH	TPG > 12 mmHg	2. PH due to left heart disease 5. PH with unclear and/or multifactorial mechanisms

Abbreviations not defined in the text: *PH*, pulmonary hypertension; *mPAP*, mean pulmonary arterial pressure; *PCWP*, pulmonary capillary wedge pressure; *DPG*, diastolic pressure gradient (diastolic PAP – mean PCWP); *PVR*, pulmonary vascular resistance; *TPG*, transpulmonary pressure gradient (mean PAP – mean PCWP); *WU*, Wood units

*All values measured at rest. **Number indicates PH group classification

Wood units are preferred to dynes s cm⁻⁵

Reproduced from Galiè et al. Eur Heart J. 2016;37:67–119, with permission of Oxford University Press on behalf of the European Society of Cardiology [25••]

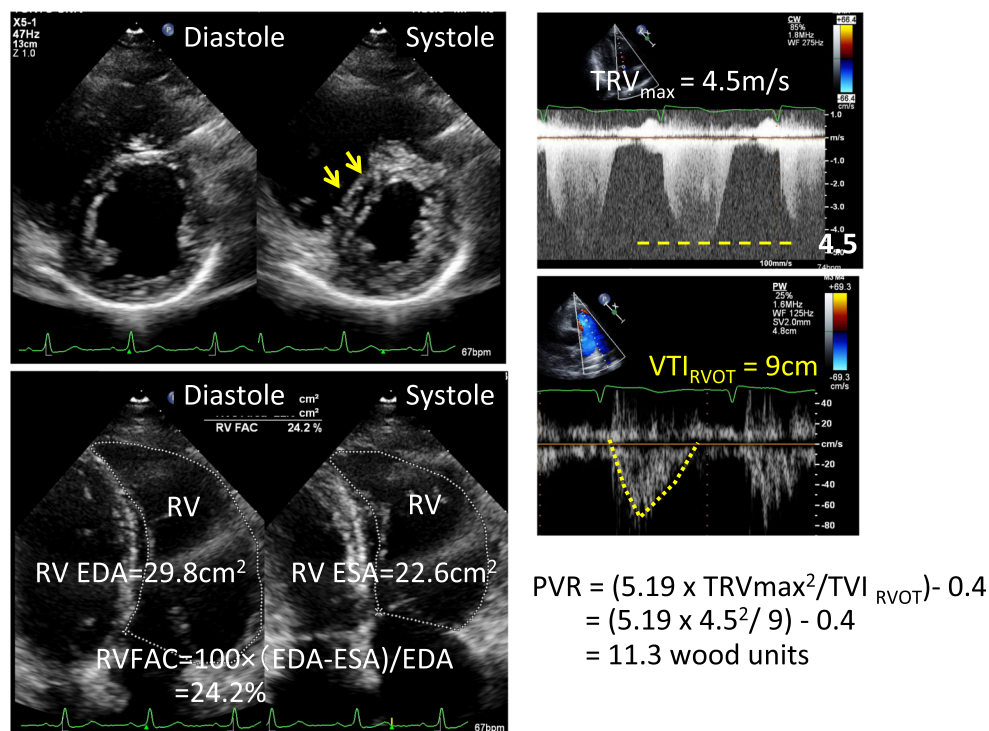


Fig. 3 Echocardiographic images obtained from a patient with a long history of left heart failure developing combined post-capillary and pre-capillary (Cpc) pulmonary hypertension. The *upper left image* demonstrates leftward septal displacement at the end-systolic phase, indicated by the yellow arrows. The *lower left image* demonstrates the reduced systolic function as reflected by low RVFAC. RVFAC $< 35\%$ indicates RV systolic dysfunction. The *right images* demonstrate the

elevation of PVR, estimated by the formula using the TRV_{max} and TVI_{RVOT}. The normal range of PVR is < 1.5 Wood units. RVFAC indicates right ventricular fractional area change; PVR indicates pulmonary vascular resistance; TRV_{max} indicates peak velocity of tricuspid regurgitation jet; TVI_{RVOT} indicates time-velocity integral of the right ventricular outflow tract

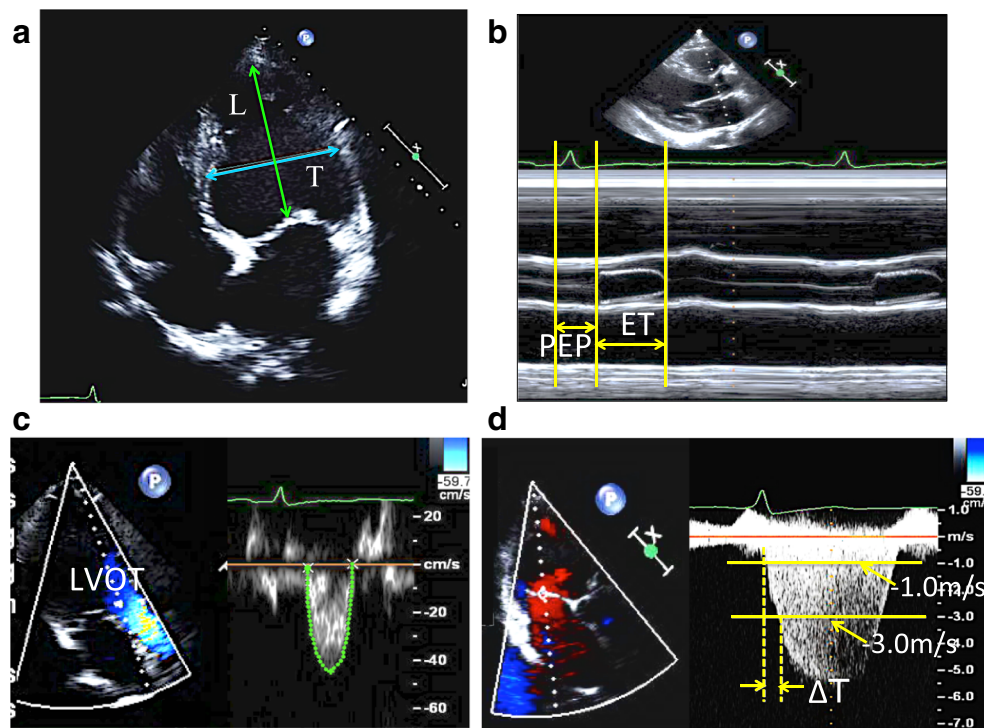


Fig. 4 **a** Sphericity index (SI). The ratio of long-axis (L) and minor-axis (T) diameters at end-diastolic phase obtained at apical four-chamber view. In patients with DCM, L/T is approximately between 1.5 and 2.0. According to the progression of LV remodeling, LV shape transforms from elliptical to spherical, and SI approaches 1, which is a sign of poor prognosis. A patient with dilated cardiomyopathy in the figure shows $L = 7.1$ cm, $T = 5.6$ cm, and $SI = 1.26$. **b** PEP/ET calculation by M-mode echocardiography at aortic valve section. PEP is the duration from Q wave of EKG to aortic opening. ET is the duration from aortic valve opening to closing. In patients with reduced LV contractility, time required for LV pressure increase is prolonged. As a result, PEP/ET increases (normal range = 0.28–0.41). The same patient in panel **a** shows PEP = 124 ms, ET = 191 ms, PEP/ET = 0.649. **c** TVI calculation by systolic forward flow at LVOT. Presuming that LVOT diameter may not alter much in each patient, the change in TVI can be used as a simple monitoring tool for CO change (normal range, 18 to 20 cm). TVI below

12 cm indicates low cardiac output. The same patient in panel **a** shows VTI = 7.47 cm. His LVOT is 2.1 cm and HR is 62 bpm, and the CO in this patient is calculated as 1.6 L/min, according to the following formula: $CO = SV$ (stroke volume) \times HR (heart rate), $SV = LVOT$ area \times TVI_{LVOT}/VTI , $LVOT$ area = $(LVOT/2)^2 \times \pi$. **d** dP/dt calculation by mitral regurgitation jet. Mitral regurgitation jet shape represents pressure gradient between LV and LA, and dP/dt is its slope. In patients with reduced LV contractility, time required for LV pressure increase is prolonged. As a result, the slope of dP/dt becomes less steep or shelving (normal range ≥ 1200 mmHg/s). In patients with severe LV systolic dysfunction, dP/dt may be below 800 mmHg/s. The calculation formula is as follows: dividing the difference of pressure gradients at 1 m/s (pressure gradient of 4 mmHg) and 3 m/s (pressure gradient of 36 mmHg) by the required time (ΔT), $dP/dt = (36 - 4) / \Delta T$. The same patient in panel **a** shows $\Delta T = 48$ s, $dP/dt = 667$ mmHg/s

Evaluation of Chamber Morphology and Patients' Prognoses by Echocardiography

In addition to the noninvasive hemodynamic assessment examined above, echocardiography is useful for obtaining both LV and RV morphological information, as well as chamber-specific functions. This information is of particular significance when attempting to risk-stratify HF patients and predict their prognoses.

Even a glance at LV shape via echocardiography aids estimation of the severity of LV remodeling and prognosis. The sphericity index is the ratio of the long-axis diameter (mitral annulus to apex at four-chamber view) and minor-axis/transverse diameter (mid-cavity level at four-chamber view or ideally at short-axis view) of the LV (Fig. 4a). This ratio can predict functional capacity in patients with LV dysfunction [27]. As compared with the LV end-diastolic dimension and LV ejection

fraction, LV volume (especially LV end-systolic volume) and LA dilatation are markers for poor prognoses [28]. Three-dimensional echocardiography can allow us to calculate LV volume as accurately as when measuring via cardiac MRI. In addition to the CO estimation using time-velocity integral (TVI) at LV outflow, serial assessment of LV contractility would help assess disease progression and responsiveness to treatment. The ratio of pre-ejection time (PEP) and ejection time (ET) of aortic valves using M-mode and dP/dt calculations using mitral regurgitation jets are also good indices for LV contractility (Fig. 4). As noted previously, LV diastolic functional analysis is also important because it presents a substantial risk for developing PH.

RV functional analysis is essential for risk stratification and prognosis assessment in patients with HF and all patients with cardiovascular diseases. The RV functional parameters, which should be obtained by echocardiography, are shown in Table 3

Table 3 Echo-derived RV parameters and their normal values

RV functional parameters		Normal values	Abnormality threshold
Systolic functional parameters	TAPSE (mm)	24 ± 3.5	< 17
	Pulsed Doppler S wave (cm/s)	14.1 ± 2.3	< 9.5
	Color Doppler S wave (cm/s)	9.7 ± 1.85	< 6.0
	RV fractional area change (%)	49 ± 7	< 35
	RV free wall 2D strain (%)	-29 ± 4.5	> -20 (absolute value < 20)
	RV 3D EF (%)	58 ± 6.5	< 45
Systolic and diastolic functional parameters	Pulsed Doppler MPI*	0.26 ± 0.085	> 0.43
	Tissue Doppler MPI	0.38 ± 0.08	> 0.54
Diastolic functional parameters	E wave deceleration time (ms)	180 ± 31	< 119 or > 242
	E/A	1.4 ± 0.3	< 0.8 or > 2.0
	e'/a'	1.18 ± 0.33	< 0.52
	e'	14.0 ± 3.1	< 7.8
	E/e	4.0 ± 1.0	> 6.0

Abbreviations not defined in the text: *MPI*, myocardial performance index (Tei index)

Reproduced and modified from Lang et al., J Am Soc Echocardiogr 2015;28:1–39, with permission from Elsevier [29]

[29]. The RV free wall lacks oblique muscle, and longitudinal contraction is a greater contributor to the RV effective stroke volume than transverse shortening [11]. Therefore, assessment of longitudinal shortening of RV as a means of RV functional analysis is logical and reliable from an anatomical point of view. Tricuspid annular plane systolic excursion (TAPSE), which quantifies the displacement of the tricuspid annular at the RV free wall, is a simple and easily obtainable parameter reflecting global RV function. Tissue Doppler imaging (TDI)-derived RV free wall *S'* [30], which is also a parameter reflecting RV longitudinal contraction, is easy to measure. Two-dimensional speckle-tracking echocardiography has also been used to evaluate RV function. A longitudinal strain of the RV free wall is a reproducible and reliable index of RV global function [31]. Interestingly, Guazzi et al. proposed that the ratio of TAPSE (reflecting RV myocardial length) and PA systolic pressure (developed pressure of RV), which indicate the cardiac “length-force relationship,” provides a comprehensive noninvasive assessment of RV contractile state and reserve [32].

Regarding the volumetric analysis of RV, two-dimensional echocardiography contains problems in its accuracy. While the LV is elliptical in shape, the RV has much complex geometry consisting of an inlet portion, an outlet portion, and an apical trabecular portion between them. Compared with the LV, the RV is more triangular or semi-lunar in form on lateral or vertical projections. As long as a patient is evaluated at an institution with sufficient experience and skills with three-dimensional echocardiography, three-dimensional echo-derived RV ejection fraction measurement is recommended as a method of quantifying RV systolic function [29].

Table 4 summarizes the echo-derived predictive indicators for prognosis in patients with HF. These parameters cannot be obtained from right heart catheterization alone and demonstrate the usefulness of concomitant assessment by cardiac imaging.

Assessment of Cardiac Function Using Cardiac Computed Tomography

Cardiac computed tomographic angiography (CTA) has been widely used as a noninvasive assessment tool of the coronary arteries, and it can detect significant coronary luminal obstruction with high accuracy. The technology of cardiac CTA using multi-detector row CT (MDCT) including submillimeter slice collimation and high temporal resolution has undergone rapid improvement. Using the raw MDCT data, we can now evaluate multiple other cardiac functional parameters, such as LV and RV volumes, ejection fractions, and cardiac output without the need for additional contrast or radiation exposure [33, 34]. Recent studies have revealed that LV volume and LVEF measurements by MDCT using retrospective gating have a good correlation with cardiac MRI, which is currently considered the gold standard for volumetric analysis [35, 36]. Regarding LV global functional analysis, MDCT is reported to be more accurate than cineventriculography, two-dimensional echocardiography, and three-dimensional echocardiography compared with MRI [36].

Cardiac CT can also be used to assess tissue characterization. The area of myocardial fibrosis or scar tissue can be detected by late enhancement (LE) in cardiac MDCT,

Table 4 Echocardiographic indices useful for predicting prognosis in patients with HF

Study	Prognostic parameters	Study results in detail	Comments
Rossi et al. (2002) [28]	DCM patients • LAVI (mL) • LVEDV (mL) • LVESV (mL) • LVEDVI (mL/m ²) • LVESVI (mL/m ²) • LVEF (%) • E/A ratio • Restrictive mitral inflow pattern • MR grade	Univariate HR (95%CI), <i>p</i> value • LAVI 1.02(1.02–1.03), <i>p</i> < 0.0001 • LVEDV 1.00(1.00–1.01), <i>p</i> = 0.001 • LVESV 1.00(1.00–1.01), <i>p</i> = 0.0003 • LVEDVI 1.01(1.00–1.01), <i>p</i> = 0.0001 • LVESVI 1.01(1.00–1.01), <i>p</i> < 0.0001 • LVEF 0.96(0.93–0.98), <i>p</i> = 0.0006 • E/A 1.6 (1.28–2.01), <i>p</i> < 0.0001 • Restrictive pattern 0.33 (0.20–0.55), <i>p</i> < 0.0001 • MR 1.21(1.028–1.44), <i>p</i> = 0.02	• LV end-systolic volume is more significantly associated with poor prognosis than LV end-diastolic volume • LV diastolic parameters and LA dilatation are more significantly associated with poor prognosis than systolic parameters
Ghio et al. (2001) [5]	Patients with LVEF < 35% • Decrease in RVFAC by 5% • NYHA (III/IV vs. II) • Increase in LVESDI by 5 mm • Increase in mPAP by 5 mmHg	Multivariate-HR (95%CI), <i>p</i> value • RVFAC 1.26 (1.10–1.46), <i>p</i> = 0.001 • NYHA 2.7 (1.4–5.1), <i>p</i> = 0.003 • LVESDI 1.20(1.04–1.40), <i>p</i> = 0.013 • mPAP 1.10 (1.0–1.21), <i>p</i> = 0.047	• RV dysfunction most significantly predicts poor prognosis
Ghio et al. (2001) [5]	• RVEF < 35% AND mPAP > 20 mmHg	• 7 times higher death/transplant; vs. RVEF > 35% AND mPAP < 20 mmHg • 3 times higher death/transplant; vs. RVEF < 35% OR mPAP > 20 mmHg	
Darahim et al. (2012) [30]	Patients with LVEF < 40% • TDI-derived RV free wall <i>S'</i> (cm/s) • TDI-derived RV <i>S'</i> integral (cm) • RVFAC (%) • TAPSE (cm)	Best cutoff value, sensitivity, specificity for death/transplant/acute HF • <i>S'</i> of 10, 92% sensitivity, 65% specificity • <i>S'</i> integral of 2.4, 80% sensitivity, 55% specificity • RVFAC of 30, 72% sensitivity, 63% specificity • TAPSE of 15.5, 75% sensitivity, 63% specificity • <i>S'</i> < 10 independently predicts poor outcomes	
Haecck ML et al. (2012) [31]	Patients with PH with any etiologies • RV longitudinal peak systolic strain \geq -19%	• Higher values cause mortality and worse NYHA functional class; vs. RV longitudinal strain < -19%	
Guazzi et al. (2013) [32]	• TAPSE/PASP < 0.36 mm/mmHg • TAPSE < 16 mm • NYHA class \geq 3 • E/e' \geq 3	Multivariate-HR (95%CI), <i>p</i> value • TAPSE/PASP 10.3 (5.4–19.8), <i>p</i> < 0.001 • TAPSE 5.1 (2.8–9.1), <i>p</i> < 0.001 • NYHA 4.4 (2.4–8.0), <i>p</i> < 0.001 • E/e' 4.1 2.3–7.2	• TAPSE/PASP independently predict cardiac death in patients with HF, irrespective of LV morphology and degree of dysfunction.

Abbreviations not defined in the text: LAVI, left atrial volume index; LVEDV, left ventricular end-diastolic volume; LVESV, left ventricular end-systolic volume; LVEDVI, left ventricular end-diastolic volume index; LVESVI, left ventricular end-systolic volume index; LVEF, left ventricular ejection fraction; MR, mitral regurgitation; EDT, mitral E wave deceleration time; LVESDI, left ventricular end-systolic diameter index; mPAP, mean pulmonary artery pressure; FMR, functional MR; TDI, tissue Doppler imaging; RV, right ventricular; RVFAC, RV fractional area change; TAPSE, tricuspid annular plane systolic excursion; NYHA, New York Heart Association

although late (or delayed) gadolinium enhancement (LGE) of cardiovascular magnetic resonance imaging (CMR) is the gold standard imaging tool of visualization in such lesions [37]. The LE detection by cardiac CT would be an alternative tool in patients with contraindications for CMR. The calculation of extracellular volume fraction (ECV) by cardiac MDCT provides useful information in the diagnosis and management of patients with cardiovascular diseases [38]. Indeed, the American College of Cardiology Foundation/American Heart Association guideline clearly states that the advantage of cardiac CT over echocardiography may be its ability to characterize the myocardium in addition to accurate assessment of cardiac structure and function [39]. Considering that low-kilovolt (KV) scans are now used to reduce radiation exposure and that automated analysis technology is rapidly improving, the role of cardiac CT for evaluating cardiac function will likely continue to be further established.

Assessment of Cardiac Function Using Cardiovascular Magnetic Resonance Imaging

The CMR can evaluate cardiac structure, morphological features, coronary narrowing, myocardial perfusion, and cardiac function using multiple imaging techniques in a single system such as spin echo imaging, gradient echo imaging, late gadolinium enhancement (LGE) sequences, and flow velocity encoding [40].

Steady-state free precession (SSFP) imaging is used for cine acquisitions to evaluate cardiac structure, wall motion, and dynamic volumetric analysis of LV and RV. It can also be useful for detecting thrombus in the cardiac chambers and clarifying the border of myocardium or prominent trabeculations, helping to diagnose noncompaction cardiomyopathy. Indeed, the assessment of chamber volume and ejection fractions by CMR is reliable and reproducible; therefore, it is now the standard noninvasive tool for cardiac functional analysis [37, 41, 42]. In

particular, the RV chamber has a complex geometry of triangular shapes with trabeculations; therefore, accurate volumetric and functional analysis by two-dimensional echocardiography contains limitations. CMR can clarify the myocardium and moving blood in a three-dimensional view, which allows adequate RV volumetric and functional analysis [42•, 43•]. Several studies have revealed the usefulness of RV functional analysis by CMR for risk stratification and prediction of prognosis in patients with PH [44, 45]. RV stroke volume is a prognostic hemodynamic parameter in PH patients, and CMR has the ability to analyze RV function [45]. RV functional analysis by CMR is now used to assess the reversibility of RV remodeling by catheter intervention in areas of chronic thromboembolic pulmonary hypertension (CTEPH) [46]. CMR-derived LA functional analysis is also a promising area for further development [47]. Diastolic functional parameters, which are equivalent to the mitral annular velocity obtained from echo-derived TDI, can also be analyzed by CMR [48].

Other CMR-related technologies of cardiac functional analysis include T1 mapping [49] and myocardial strain measurements [50]. T1 myocardial mapping can be performed either with or without gadolinium-based contrast agents. T1 mapping without or before contrast administration is called native T1 mapping, which reflects the myocardial disease tissue-specific and interstitial changes. Using post-contrast T1 mapping and native T1 mapping together with the hematocrit level measurement, ECV fraction can be calculated [49]. Myocardial strain analysis by CMR is useful for both global and regional myocardial functional evaluation. Several methodologies have been applied, including CMR tagging, phase velocity mapping (PVM), displacement encoding with simulated echoes (DENCE), and strain encoded (SENC). Recently developed CMR feature tracking (CMR-FT) uses similar methodology to speckle-tracking echocardiography and analyzes results with a post-processing approach to existing data without additional image acquisition [50]. In patients who have limited transthoracic echocardiographic windows, CMR-FT is a useful tool for evaluating global and local myocardial function by strain measurement.

Conclusion

Echocardiography can be performed serially at the bedside, and some key parameters are relatively easily obtainable; thus, it can be a valid alternative to invasive cardiac catheterization and suitable for hemodynamic monitoring. Complex parameters of pulmonary hemodynamics can also be evaluated by echocardiography. Cardiac CT and CMR are used not only for global cardiac functional analysis but also for evaluation of myocardial tissue and interstitial characterization.

Cardiac imaging modalities, when several tools are combined, can provide hemodynamic information, including

pulmonary circulation as well as structure and morphological feature of the cardiac chambers in a comprehensive manner.

Funding Information This work is partially supported by Japan Society for the Promotion of Science (JSPS) KAKENHI Grant-in-Aid for Scientific Research C (Grant Number 16K09454) to Dr. Kato.

Compliance with Ethical Standards

Conflict of Interest Tomoko S. Kato, Masao Daimon, and Toru Satoh declare that they have no conflict of interest.

Human and Animal Rights and Informed Consent This article does not contain any studies with human or animal subjects performed by any of the authors.

References

Papers of particular interest, published recently, have been highlighted as:

- Of importance
- Of major importance

1. Lesyuk W, Kriza C, Kolominsky-Rabas P. Cost-of-illness studies in heart failure: a systematic review 2004-2016. *BMC Cardiovasc Disord.* 2018;18:74.
2. Ambrosy AP, Fonarow GC, Butler J, Chioncel O, Greene SJ, Vaduganathan M, et al. The global health and economic burden of hospitalizations for heart failure: lessons learned from hospitalized heart failure registries. *J Am Coll Cardiol.* 2014;63:1123–33.
3. Chaudhry SI, Mattera JA, Curtis JP, Spertus JA, Herrin J, Lin Z, et al. Telemonitoring in patients with heart failure. *N Engl J Med.* 2010;363:2301–9. <https://doi.org/10.1056/NEJMoa1010029>.
4. Adamson PB, Ginn G, Anker SD, Bourge RC, Abraham WT. Remote haemodynamic-guided care for patients with chronic heart failure: a meta-analysis of completed trials. *Eur J Heart Fail.* 2017;19:426–33.
5. Ghio S, Gavazzi A, Campana C, Inserra C, Klersy C, Sebastiani R, et al. Independent and additive prognostic value of right ventricular systolic function and pulmonary artery pressure in patients with chronic heart failure. *J Am Coll Cardiol.* 2001;37:183–8.
6. Abraham WT, Adamson PB, Bourge RC, Aaron MF, Costanzo MR, Stevenson LW, et al. *Lancet.* 2011;377:658–66.
7. Kalogeropoulos AP, Siwamogsatham S, Hayek S, Li S, Deka A, Marti CN, et al. Echocardiographic assessment of pulmonary artery systolic pressure and outcomes in ambulatory heart failure patients. *J Am Heart Assoc.* 2014;3:e000363.
8. Aronson D, Eitan A, Dragu R, Burger AJ. Relationship between reactive pulmonary hypertension and mortality in patients with acute decompensated heart failure. *Circ Heart Fail.* 2011;4:644–50.
9. Haddad F, Doyle R, Murphy DJ, Hunt SA. Right ventricular function in cardiovascular disease, part II: pathophysiology, clinical importance, and management of right ventricular failure. *Circulation.* 2008;117:1717–31.
10. Abel FL, Waldhausen JA. Effects of alterations in pulmonary vascular resistance on right ventricular function. *J Thorac Cardiovasc Surg.* 1967;54:886–94.
11. Brown SB, Raina A, Katz D, Szerlip M, Wieggers SE, Forfia PR. Longitudinal shortening accounts for the majority of right ventricular contraction and improves after pulmonary vasodilator therapy

- in normal subjects and patients with pulmonary arterial hypertension. *Chest*. 2011;140:27–33.
12. Meyer P, Filippatos GS, Ahmed MI, Iskandrian AE, Bittner V, Perry GJ, et al. Effects of right ventricular ejection fraction on outcomes in chronic systolic heart failure. *Circulation*. 2010;121:252–8.
 13. Porter TR, Shillcutt SK, Adams MS, Desjardins G, Glas KE, Olson JJ, et al. Guidelines for the use of echocardiography as a monitor for therapeutic intervention in adults: a report from the American Society of Echocardiography. *J Am Soc Echocardiogr*. 2015;28:40–56 **This is the most recent guideline for the use of echocardiography as a noninvasive hemodynamic monitoring tool.**
 14. Beigel R, Cercek B, Luo H, Siegel RJ. Noninvasive evaluation of right atrial pressure. *J Am Soc Echocardiogr*. 2013;26:1033–42.
 15. Beigel R, Cercek B, Arsanjani R, Siegel RJ. Echocardiography in the use of noninvasive hemodynamic monitoring. *J Crit Care*. 2014;29:184.e1–8.
 16. Temporelli PL, Scapellato F, Eleuteri E, Imparato A, Giannuzzi P. Doppler echocardiography in advanced systolic heart failure: a non-invasive alternative to Swan-Ganz catheter. *Circ Heart Fail*. 2010;3:387–94.
 17. Abbas AE, Franey LM, Marwick T, Maeder MT, Kaye DM, Vlahos AP, et al. Noninvasive assessment of pulmonary vascular resistance by Doppler echocardiography. *J Am Soc Echocardiogr*. 2013;26:1170–7.
 18. Nagueh SF, Appleton CP, Gillebert TC, Marino PN, Oh JK, Smiseth OA, et al. Recommendations for the evaluation of left ventricular diastolic function by echocardiography, vol. 10; 2009. p. 165–93.
 19. Abbas AE, Fortuin FD, Patel B, Moreno CA, Schiller NB, Lester SJ. Noninvasive measurement of systemic vascular resistance using Doppler echocardiography. *J Am Soc Echocardiogr*. 2004;17:834–8.
 20. Magnin PA, Stewart JA, Myers S, VonRamm O, Kisslo JA. Combined Doppler and phased-array echocardiographic estimation of cardiac output. *Circulation*. 1981;63:388–92.
 21. Kato TS, Nishimura T, Kyo S, Kuwaki K, Dada H, Amano A. The role of echocardiography in the management of patients undergoing a ventricular assist device implantation and/or transplantation. *Echocardiography in heart failure and cardiac electrophysiology*. In: Lakshmanadoss U, editor. *Echocardiography in heart failure and cardiac electrophysiology*. London: IntechOpen Inc; 2016. <https://doi.org/10.5772/65095>.
 22. Greiner S, Jud A, Aurich M, Hess A, Hilbel T, Hardt S, et al. Reliability of noninvasive assessment of systolic pulmonary artery pressure by Doppler echocardiography compared to right heart catheterization: analysis in a large patient population. *J Am Heart Assoc*. 2014;3:e001103.
 23. Lam CS, Borlaug BA, Kane GC, Enders FT, Rodeheffer RJ, Redfield MM. Age-associated increases in pulmonary artery systolic pressure in the general population. *Circulation*. 2009;119:2663–70.
 24. Kalogeropoulos AP, Georgiopoulou VV, Borlaug BA, Gheorghiadu M, Butler J. Left ventricular dysfunction with pulmonary hypertension: part 2: prognosis, noninvasive evaluation, treatment, and future research. *Circ Heart Fail*. 2013;6:584–93.
 25. Galiè N, Humbert M, Vachiery JL, Gibbs S, Lang I, Torbicki A, et al. ESC Scientific Document Group. 2015 ESC/ERS Guidelines for the diagnosis and treatment of pulmonary hypertension: Joint Task Force for the Diagnosis and Treatment of Pulmonary Hypertension of the European Society of Cardiology (ESC) and the European Respiratory Society (ERS): endorsed by: Association for European Paediatric and Congenital Cardiology (AEPC), International Society for Heart and Lung Transplantation (ISHLT). *Eur Heart J*. 2016;37:67–119 **These latest international guidelines establish the diagnostic algorithm and treatment for pulmonary hypertension.**
 26. Gómez A, Bialostozky D, Zajarias A, Santos E, Palomar A, Martínez ML, et al. Right ventricular ischemia in patients with primary pulmonary hypertension. *Am Coll Cardiol*. 2001;38:1137–42.
 27. Tischler MD, Niggel J, Borowski DT, LeWinter MM. Relation between left ventricular shape and exercise capacity in patients with left ventricular dysfunction. *J Am Coll Cardiol*. 1993;22:751–7.
 28. Rossi A, Cicoira M, Zanolta L, Sandrini R, Golia G, Zardini P, et al. Determinants and prognostic value of left atrial volume in patients with dilated cardiomyopathy. *J Am Coll Cardiol*. 2002;40:1425–30.
 29. Lang RM, Badano LP, Mor-Avi V, Afilalo J, Armstrong A, Ernande L, et al. Recommendations for cardiac chamber quantification by echocardiography in adults: an update from the American Society of Echocardiography and the European Association of Cardiovascular Imaging. *J Am Soc Echocardiogr*. 2015;28:1–39.
 30. Darahim KE. Right ventricular systolic echocardiographic parameters in chronic systolic heart failure and prognosis. *Egyptian Heart J*. 2014;66:317–25.
 31. Haeck ML, Scherptong RW, Marsan NA, Holman ER, Schalij MJ, Bax JJ, et al. Prognostic value of right ventricular longitudinal peak systolic strain in patients with pulmonary hypertension. *Circ Cardiovasc Imaging*. 2012;5:628–36.
 32. Guazzi M, Bandera F, Pelissero G, Castelvechio S, Menicanti L, Ghio S, et al. Tricuspid annular plane systolic excursion and pulmonary arterial systolic pressure relationship in heart failure: an index of right ventricular contractile function and prognosis. *Am J Physiol Heart Circ Physiol*. 2013;305:H1373–81.
 33. Butler J. The emerging role of multi-detector computed tomography in heart failure. *J Cardiac Fail*. 2007;13:215–26.
 34. Singh RM, Singh BM, Mehta JL. Role of cardiac CTA in estimating left ventricular volumes and ejection fraction. *World J Radiol*. 2014;6:669–76.
 35. Kara B, Nayman A, Guler I, Gul EE, Koplay M, Paksoy Y. Quantitative assessment of left ventricular function and myocardial mass: a comparison of coronary CT angiography with cardiac MRI and echocardiography. *Pol J Radiol*. 2016;81:95–102.
 36. Greupner J, Zimmermann E, Grohmann A, Dübel HP, Althoff TF, Borges AC, et al. Head-to-head comparison of left ventricular function assessment with 64-row computed tomography, biplane left cineventriculography, and both 2- and 3-dimensional transthoracic echocardiography: comparison with magnetic resonance imaging as the reference standard. *J Am Coll Cardiol*. 2012;59:1897–907.
 37. Langer C, Lutz M, Eden M, Lüdde M, Hohnhorst M, Gierloff C, et al. Hypertrophic cardiomyopathy in cardiac CT: a validation study on the detection of intramyocardial fibrosis in consecutive patients. *Int J Cardiovasc Imaging*. 2014;30:659–67.
 38. Treibel TA, Fontana M, Maestrini V, Castelletti S, Rosmini S, Simpson J, et al. Automatic measurement of the myocardial interstitium: synthetic extracellular volume quantification without hematocrit sampling. *JACC Cardiovasc Imaging*. 2016;9:54–63.
 39. WRITING COMMITTEE MEMBERS, Yancy CW, Jessup M, Bozkurt B, Butler J, Casey DE Jr, et al. 2013 ACCF/AHA guideline for the management of heart failure: a report of the American College of Cardiology Foundation/American Heart Association Task Force on practice guidelines. *Circulation*. 2013;128:e240–327.
 40. Pennell DJ, Sechtem UP, Higgins CB, Manning WJ, Pohost GM, Rademakers FE, et al. Clinical indications for cardiovascular magnetic resonance (CMR): consensus panel report. *Eur Heart J*. 2004;25:1940–65.
 41. Bellenger NG, Burgess MI, Ray SG, Lahiri A, Coats AJ, Cleland JG, et al. Comparison of left ventricular ejection fraction and volumes in heart failure by echocardiography, radionuclide

- ventriculography and cardiovascular magnetic resonance; are they interchangeable? *Eur Heart J*. 2000;21:1387–96.
42. Peterzan MA, Rider OJ, Anderson LJ. The role of cardiovascular magnetic resonance imaging in heart failure. *Card Fail Rev*. 2016;2:115–22. <https://doi.org/10.15420/cfr.2016.2.2.115> **This paper nicely summarizes the usefulness of cardiovascular magnetic resonance imaging in the care of heart failure patients and its future perspective.**
 43. Grothues F, Moon JC, Bellenger NG, Smith GS, Klein HU, Pennell DJ. Interstudy reproducibility of right ventricular volumes, function, and mass with cardiovascular magnetic resonance. *Am Heart J*. 2004;147:218–23.
 44. van Wolferen SA, van de Veerdonk MC, Mauritz GJ, Jacobs W, Marcus JT, Marques KMJ, et al. Clinically significant change in stroke volume in pulmonary hypertension. *Chest*. 2011;139:1003–9.
 45. van Wolferen SA, Marcus JT, Boonstra A, Marques KM, Bronzwaer JG, Spreeuwenberg MD, et al. Prognostic value of right ventricular mass, volume, and function in idiopathic pulmonary arterial hypertension. *Eur Heart J*. 2007;28:1250–7.
 46. Fukui S, Ogo T, Morita Y, Tsuji A, Tateishi E, Ozaki K, et al. Right ventricular reverse remodelling after balloon pulmonary angioplasty. *Eur Respir J*. 2014;43:1394–402.
 47. Habibi M, Chahal H, Opdahl A, Gjesdal O, Helle-Valle TM, Heckbert SR, et al. Association of CMR-measured LA function with heart failure development: results from the MESA study. *JACC Cardiovasc Imaging*. 2014;7:570–9.
 48. Wu V, Chyou JY, Chung S, Bhagavatula S, Axel L. Evaluation of diastolic function by three-dimensional volume tracking of the mitral annulus with cardiovascular magnetic resonance: comparison with tissue Doppler imaging. *J Cardiovasc Magn Reson*. 2014;16:71.
 49. Moon JC, Messroghli DR, Kellman P, Piechnik SK, Robson MD, Ugander M, et al. Myocardial T1 mapping and extracellular volume quantification: a Society for Cardiovascular Magnetic Resonance (SCMR) and CMR Working Group of the European Society of Cardiology consensus statement. *J Cardiovasc Magn Reson*. 2013;14(15):92.
 50. Scatteia A, Baritussio A, Bucciarelli-Ducci C. Strain imaging using cardiac magnetic resonance. *Heart Fail Rev*. 2017;22:465–76.

Publisher's Note Springer Nature remains neutral with regard to jurisdictional claims in published maps and institutional affiliations.